Materials Research Bulletin 134 (2021) 111118

Contents lists available at ScienceDirect

Materials Research Bulletin

journal homepage: www.elsevier.com/locate/matresbu

Unidirectional crystal growth of L-alanine doped triglycine sulphate crystals along [010] polar direction in ferroelectric and paraelectric temperature ranges, and their comparative characterizations

Muthu Senthil Pandian [a,*], Sunil Verma [b,c], P. Karuppasamy [a], P. Ramasamy [a], V.S. Tiwari [b,c], A. K. Karnal [b,c]

[a] Research Centre, Sri Sivasubramaniya Nadar College of Engineering, Chennai, 603110, Tamilnadu, India
[b] Laser & Functional Materials Division, Raja Ramanna Centre for Advanced Technology, Indore, 452013, Madhya Pradesh, India
[c] Homi Bhabha National Institute, BARC Training School Complex, Anushakti Nagar, Mumbai, 400094, Maharashtra, India

ARTICLE INFO

Keywords:
Crystal growth from solution
TGS-Ferroelectric crystal
Curie temperature
Electrical properties
Optical transmission

ABSTRACT

Good quality, large size (010) polar face oriented ferroelectric single crystals of L-alanine doped triglycine sulphate (LA-TGS) were grown by unidirectional solution growth technique in two temperature regimes on either side of its Curie temperature (T_c). The growth conditions were optimized to obtain LA-TGS crystals of length = 40 mm, diameter = 30 mm below Curie temperature (T_c), and length = 50 mm, diameter = 15 mm above Curie temperature, with growth rates of 1.3 and 3.0 mm/day, respectively. Powder XRD was performed for phase confirmation and DTA for phase transition temperature determination, and compared with data of undoped TGS crystal. Crystal grown below T_c has almost same dislocations density, two times higher piezoelectric d_{33} coefficient, and three times lower dielectric permittivity as compared to the crystal grown above T_c, showing its better device potential. The UV-Vis-NIR transmittance of the two crystals was ≥80 %, showing their good optical quality.

1. Introduction

In recent years, ferroelectric materials have been the subject of growing interest due to their widespread technological applications in electronic and optoelectronic devices as well as their potential application in high-density data storage [1]. TGS ($(NH_2CH_2COOH)_3.H_2SO_4$) is one of the important ferroelectric crystals for infrared (IR) detection applications mainly because of its features which allow operation at room temperature. For the fabrication of IR detectors and laser energy meter applications, large area (010) plates of specifically doped TGS crystals are required [2,3]. Crystals of the TGS family have also been used as target materials in the manufacturing of pyroelectric VIDICON tubes [4]. Electron emission from TGS crystals, stimulated by polarization switching, has been reported as suitable for electron gun devices [5]. TGS undergoes a second-order phase transition at Curie temperature (49.3 °C) from ferroelectric to paraelectric phase. The crystal system of TGS is monoclinic at temperatures below and above its Curie temperature, but the space group transforms from non-centrosymmetric $P2_1$ in the ferroelectric phase to centrosymmetric $P2_1/m$ in the paraelectric phase.

One of the major drawbacks of TGS crystal, when used as a pyroelectric detector element for IR array, is the depolarization with time leading to a decrease in the efficiency of devices over time. An effective way to stabilize the single domain state is by doping an optically active molecule into TGS. The partial substitution of an optically active molecule in the place of a glycine molecule causes an internal bias field, which makes the crystal permanently polarized [6]. To modify and improve the properties of TGS for device applications, a wide range of organic, inorganic, and metallic dopants have been attempted [7–9] to inhibit the ferroelectric switching to increase crystal unipolarity and hence the resulting figure of merit. Some of the dopants were found to prevent thermal depoling and also shift the Curie point to a higher temperature. The substitution of L-alanine in TGS has been found to improve the physical properties by contributing to an effective internal bias in these crystals. For this reason, L-alanine doped TGS family crystals have been investigated by many researchers [10–13].

Several works have been reported on the doping of L-alanine in TGS (LA-TGS) crystals by the conventional slow evaporation method. The

* Corresponding author at: Tel.: +91-9944294169.
E-mail addresses: senthilpandianm@ssn.edu.in (M.S. Pandian), sverma1118@gmail.com (S. Verma).

https://doi.org/10.1016/j.materresbull.2020.111118
Received 28 April 2020; Received in revised form 22 October 2020; Accepted 26 October 2020
Available online 31 October 2020

drawback of conventional method grown LA-TGS crystal, having natural morphology, as well as those grown preferentially along specific crystallographic directions, is that the crystal has to be cut and polished along specific (010) face to get an element suitable for IR devices. This results in a very small portion of the grown crystal usable for practical device applications. SR growth method provides a solution to this limitation of the conventional growth method by enabling growth along device relevant directions, which increases the device purpose yield of the crystal [14]. Unidirectional [001] and [010] pure TGS crystals have been already grown by the SR method and the comparative characterizations were reported in earlier investigations by the authors [15,16]. Recently, authors have reported SR growth of pure and Urea doped TGS crystals along [010] direction in paraelectric and ferroelectric temperature ranges [17,18]. However, growth of L-alanine doped TGS crystal by unidirectional SR method along [010] direction in temperatures above and below its phase transition temperature, and subsequent investigations of their device relevant physical properties has not been reported in the literature so far, which are the aims of the present paper. The growth of LA-TGS in ferroelectric temperature range has been performed at 37 °C, while the growth in paraelectric temperature range has been performed at 57 °C. In the present investigation, the LA-TGS crystals grown below and above T_c were subjected to the growth rate analysis, structural characterization, thermal studies, defects density, piezoelectric, dielectric and optical studies. The physical properties and crystalline perfection of LA-TGS crystals have been investigated systematically for the first time. The results establish specific relationship between the physical properties and crystalline quality of LA-TGS crystals grown in ferroelectric and paraelectric phases. The results also provide insight into the fundamental relationships between the growth rates, physical properties, point defects, and the resulting ferroelectric properties.

2. Unidirectional crystal growth of L-alanine doped triglycine sulphate (LA-TGS)

2.1. [010] seed crystal from conventionally grown crystal

TGS was synthesized by taking GR grade glycine (NH_2CH_2COOH) and concentrated sulfuric acid (H_2SO_4) in the molar ratio of 3:1. The required volume of concentrated sulfuric acid was diluted with Millipore water of resistivity 18.2 MΩ cm. Then the calculated amount of glycine material was slowly dissolved in the diluted sulfuric acid. To this mixture 7 mol % of L-alanine was added. This solution was heated continuously until the solvent evaporated and LA-TGS material crystallized at the bottom. The crystallized material was again dissolved in Millipore water and then recrystallized. The 7 mol % L-alanine doped TGS solution saturated at 30 °C was prepared. It was overheated to 35 °C for about 10 h and filtered using 0.2 μm membrane filter to eliminate the extraneous solid colloidal particles that can be possible sources of spontaneous nucleation. The filtered solution was poured into a glass beaker and covered by a plastic membrane sheet having fine perforations. It was then placed in a constant temperature bath at the saturation temperature of 30 °C. The solubility of pure TGS at the temperature of 30 °C is 36 g/100 mL. But the solubility of L-alanine doped TGS at 30 °C is 43 g/100 mL and at 57 °C is 75 g/100 mL. A small spontaneously nucleated crystal started to grow in the crystallizer. After three weeks of growth, the natural morphology crystal was obtained from the crystallizer. The morphology of the conventionally-grown LA-TGS is shown in Fig. 1, along with the methodology to cut the crystal to obtain seed crystal oriented along [010] to initiate growth along the polar direction using unidirectional solution growth method.

2.2. Experimental set up for unidirectional crystal growth by SR method

The schematic diagram of the SR method is shown in Fig. 2. The unidirectional crystal growth apparatus consists of two long glass beakers of 30 cm height and diameters 12 cm and 30 cm. The temperature of the constant temperature water bath, in which the unidirectional growth apparatus was kept, was maintained by temperature controlling instrumentation consisting of "U" shaped heaters, RTD temperature sensors (PT100), PID controllers (Eurotherm 902P model), and thyristors (Eurotherm 415A model) within the stability of ±0.01 °C. The lower half of the smaller diameter beaker was immersed in water inside the bigger beaker, while the upper half had a nichrome strip heater covered with silica-glass wool for thermal insulation. A borosilicate glass ampoule of length 150 mm with conical tip was fabricated and cleaned using acetone. Natural morphology TGS crystal obtained by the conventional slow cooling method was cut perpendicular to polar b-axis and made into a conical shape to fix at the conical bottom of the ampoule using silicone paste. A 30 mm thick Plexiglas circular plate was used to cover the top portion of the ampoule to avoid evaporation of solution from the crystallizer. A glass container was placed over the ampoule as a protective hood. The entire setup was sealed and placed in a dust-free environment. The unidirectional crystal growth set up along with the PID temperature control instrumentation for experiments below and above T_c is shown in Fig. 3. A spiral ring heater was placed around the bottom and top portions of the growth ampoule and connected to separate temperature controlling instrumentation, which provided the necessary temperature stability near to the seed crystal during growth. The top portion was maintained at a higher temperature for solvent

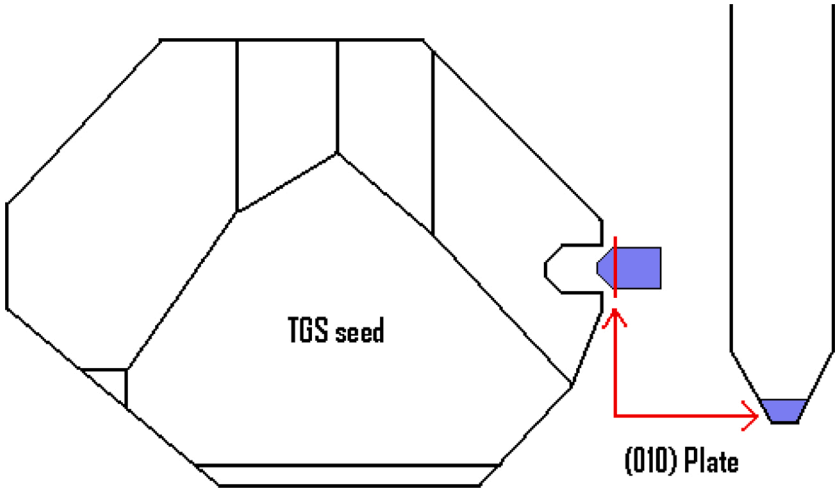

Fig. 1. Morphology of conventionally grown LA-TGS crystal, and methodology to obtain [010] oriented seed crystal for unidirectional growth.

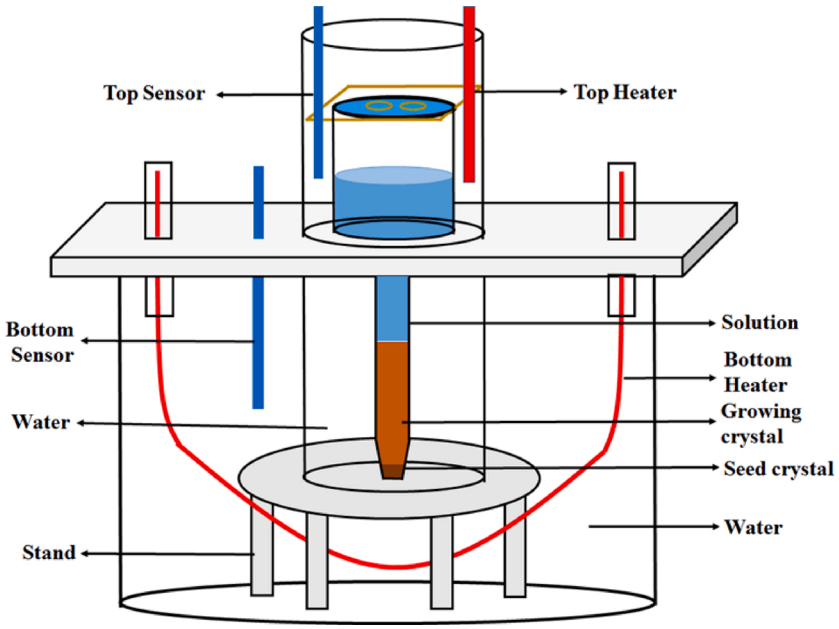

Fig. 2. Schematic of unidirectional solution growth system.

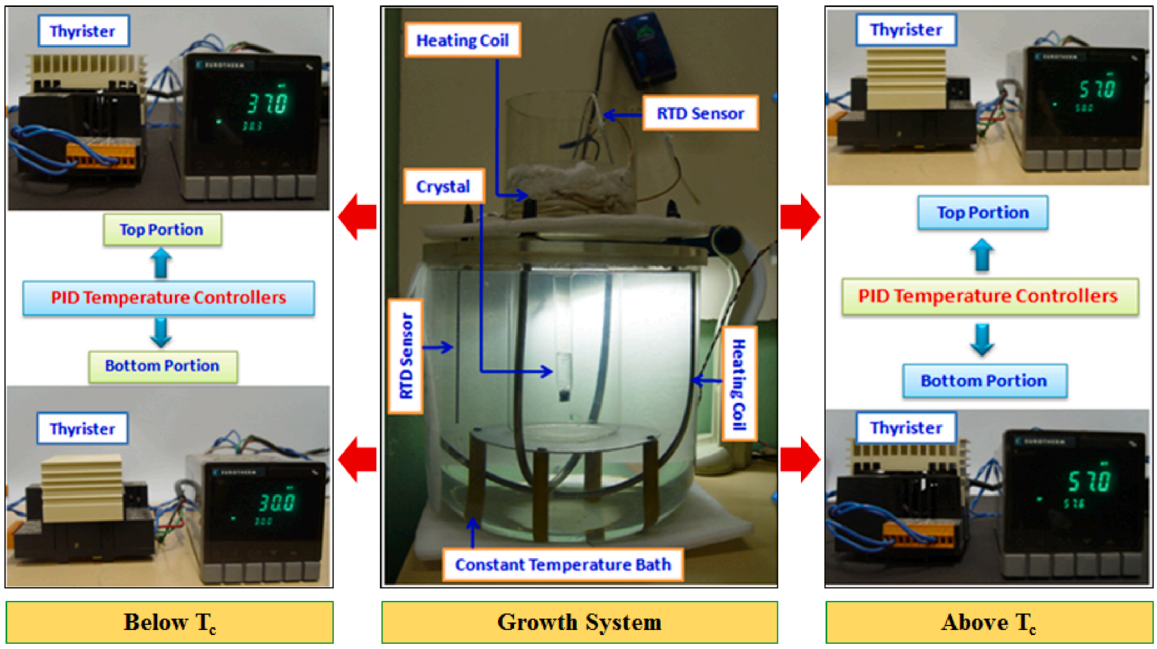

Fig. 3. Experimental set up for unidirectional solution growth and associated PID temperature control instrumentation for LA-TGS crystal growth below and above T_c.

evaporation. The evaporation rate was empirically controlled by using different pore sizes in the Plexiglas lid, which was covered by a semi-permeable membrane that allows passage of solvent vapors. The growth condition of this method depends on the temperatures of the top and bottom portions of the ampoule. This experimental set up was used for the SR growth of LA-TGS crystal in ferroelectric and paraelectric temperature ranges along the [010] polar axis.

2.3. Unidirectional growth of LA-TGS crystal below T_c along [010] direction

The crystals were grown by controlled slow evaporation of the solvent, which resulted in a supersaturated solution, which was maintained constant empirically by observing the decrease in the level of the solution in the ampoule. This in-turn results in constant supersaturation inside the crystallizer, which leads to crystal growing at a constant growth rate. This is further supported by the fact that due to gravity-driven mass transfer in the SR growth, a constant flux of growth units is maintained towards the growing crystal surface, and hence no fluctuation in supersaturation is observed, which manifests itself in the uniform growth rate of the crystal [19]. The optimized temperature profiles of the top and bottom regions of ampoule during the growth of LA-TGS crystal below T_c were 37 °C in the top and 30 °C in the bottom portion. Fig. 4(a) shows the growing single crystal of LA-TGS. The total growth period was 30 days. The as-grown transparent crystal of length = 40 mm and diameter = 30 mm, and the cut and polished (010)

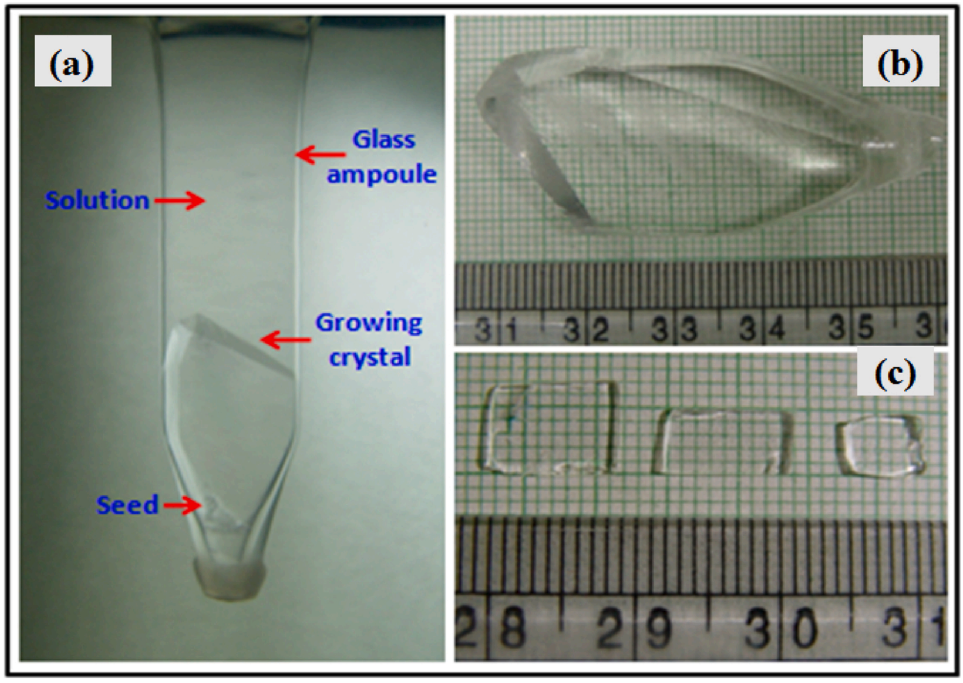

Fig. 4. (a) LA-TGS crystal growing below T_c inside the ampoule, (b) as-grown LA-TGS crystal grown below T_c and (c) polished (010) wafers from the LA-TGS crystal grown below T_c.

wafers of the LA-TGS crystal are shown in Fig. 4(b, c) respectively. The growth rate of the LA-TGS crystals grown along [010] polar direction was measured from the time-lapsed photographs of the crystal growth process taken at a regular interval of time. The time-lapsed photos after 3, 8, 17, and 30 days of growth are shown in Fig. 6(a). The solid-liquid interface was always the (010) face. The plot of growth rate as a function of the growth period (Fig. 7(a)) shows that the average growth rate was 1.3 mm/day.

2.4. Unidirectional growth of LA-TGS crystal above T_c along [010] direction

Several growth runs were performed by trying various temperatures for the top and bottom regions of the growth ampoule, and the optimized temperature for the two regions of the ampoule for growth in the paraelectric temperature range was 57 °C. The parameters used for optimizing the growth temperature in the paraelectric phase were

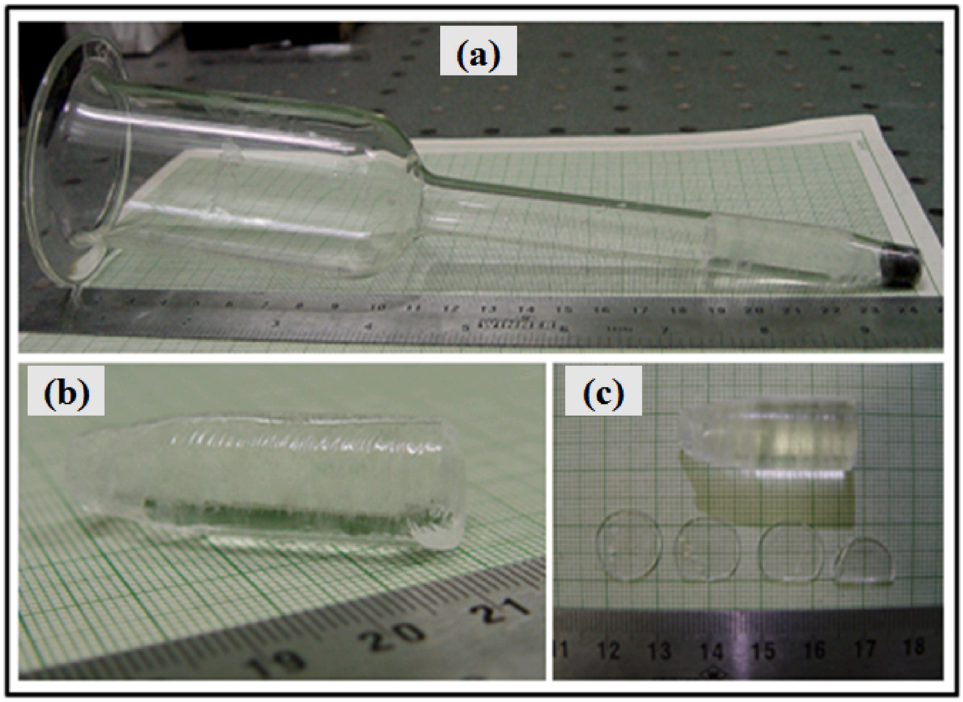

Fig. 5. (a) LA-TGS crystal grown above T_c inside the ampoule, (b) as-grown LA-TGS crystal grown above T_c and (c) cut and polished (010) wafers from the LA-TGS crystal grown above T_c.

solubility, growth system design, quality of the growing crystal, and the growth rate. Above as well as below this optimized value of 57 °C, several defects such as spurious nucleation, cracks, and inclusions were observed in the crystal. The experimental apparatus showing optimized growth parameters during growth in paraelectric temperature range is shown in Fig. 3. Highly transparent crystal of LA-TGS of length = 50 mm and diameter = 15 mm was grown in a period of 17 days. The grown crystal inside the ampoule and after removing it from the ampoule is shown in Fig. 5(a, b) respectively. After completion of the growth experiment, the solution from the ampoule was removed using a glass pipette, and thereafter the temperature of the thermostatic bath was slowly cooled to room temperature at a rate of 1 °C/hr, to avoid any thermal shock. The cut and polished (010) wafers from the grown LA-TGS crystal are shown in Fig. 5(c). The growth rate of the crystal was calculated by recording the growth process at a regular interval of period. Fig. 6(b) shows the time-lapse photographs of the LA-TGS crystal growing at 57 °C after 3, 5, 10, 12, 15, and 17 days of growth. The plot of growth rate as a function of the time period of growth (in days) is shown in Fig. 7(b). The graph clearly shows that the growth rate of LA-TGS crystal grown above T_c was ~ 3 mm/day. It may be noted that although the growth rate of crystal grown above T_c is approximately twice as compared to that of below T_c grown crystal, the diameter of crystal was half as compared to that grown below T_c. So, the two crystals were grown with approximately the same rate of crystallization.

3. Sample fabrication for characterization of LA-TGS crystals

Samples of LA-TGS single crystals grown by unidirectional SR method were cleaved perpendicular to the b-axis to get (010) slices of identical thickness. The samples were polished using a mixture of ethylene glycol and alumina powder to remove scratches and other mechanical damages on surfaces that occur during cleavage. The comparative characterizations were performed on LA-TGS crystals grown in ferroelectric and paraelectric temperature ranges. Wherever possible, the characterization was repeated to confirm the reproducibility of results.

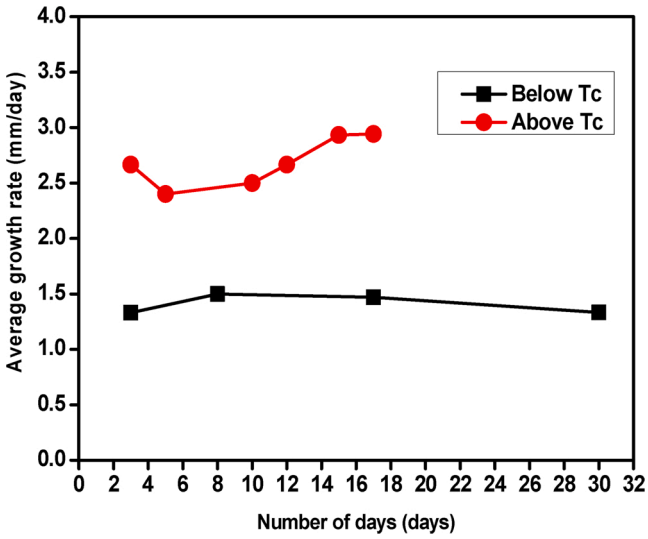

Fig. 7. Average growth rate versus growth period for crystal grown below and above T_c.

3.1. Powder X-ray diffraction (PXRD)

To confirm the phase of pure and L-alanine doped TGS crystal, the powder x-ray diffraction was performed using the Rigaku Geigerflex diffractometer with CuK_α (1.5405 Å) radiation. The specimen was scanned in reflection mode in the 2θ range from 10° to 70° with a scan speed of 2°/min. Good agreement between the experimental and literature parameters was obtained. The compound has monoclinic structure at room temperature with a =9.413 Å, b =12.645 Å, c =5.735 Å. All the observed prominent peaks in XRD patterns are indexed as shown in Fig. 8(a, b) for doped and pure TGS, respectively. It is observed that there is a slight variation in the intensity of peaks in the powder XRD of the two crystals, but their position is the same. The relative change in the intensities of the reflection peaks corresponding to (040), (211), (231), (150), and (101) may be attributed to the introduction of point defects in the lattice due to the dopant L-alanine.

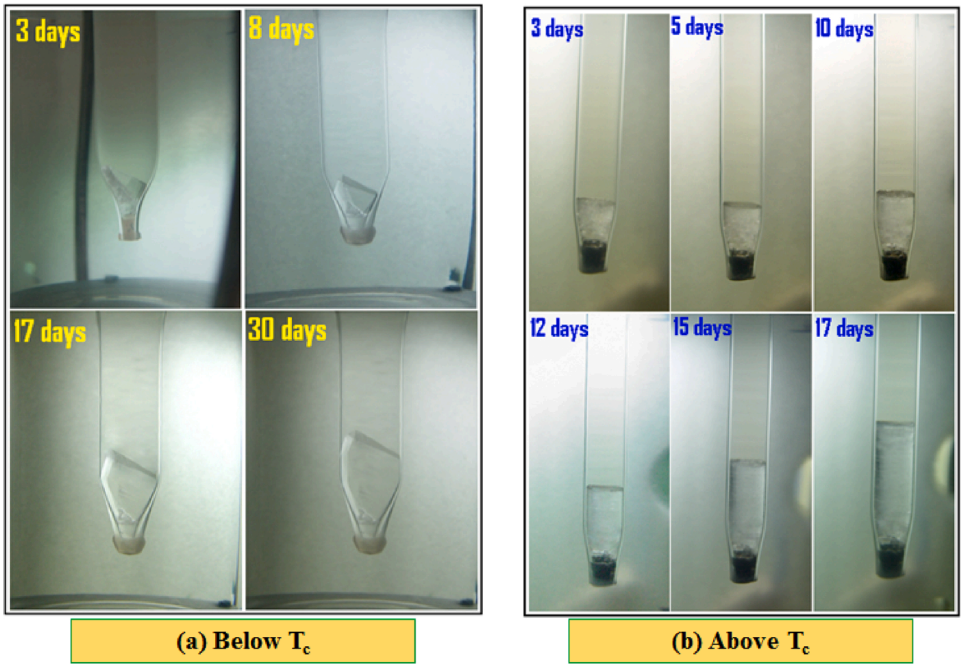

Fig. 6. Day wise growth of LA-TGS crystal grown (a) below T_c and (b) above T_c (day of growth is mentioned on the respective image).

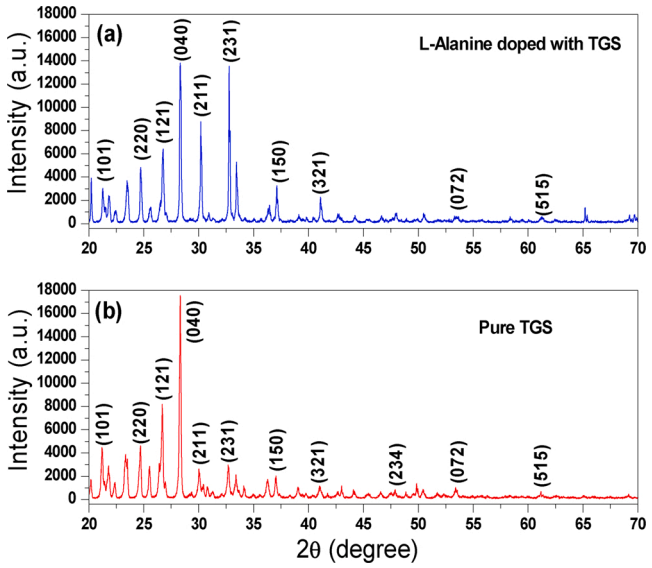

Fig. 8. Powder XRD of (a) LA-TGS crystal grown below T_c and (b) pure TGS crystal.

3.2. Phase transition and differential thermal analysis

Differential thermal analysis (DTA) of pure and LA-TGS crystal was carried out between 30–250 °C at a heating rate of 10 °C/min in a nitrogen atmosphere. Fine powder samples were weighed in a platinum crucible. A comparative DTA curve of pure and L-alanine doped crystal is presented in Fig. 9(b). From the curve, the endothermic peak is observed, which shows that phase transition in pure and LA-TGS crystal occurs at 50 °C and 52 °C, respectively. The change in phase transition temperature of LA-TGS crystal may be attributed to the fact that the L-alanine dopant alters the bonding environment between polar units in the TGS, which results in a change in the temperature up to which ferroelectricity is observed. The DTA curve of pure and LA-TGS crystal shown in Fig. 9(a) indicate endothermic peaks at 226 °C and 216 °C, representing decomposition. There is no exothermic or endothermic peaks below 216 °C of the sample, indicating that the crystal is moisture free and stable up to 216 °C. Based on this study, it can be said that the LA-TGS crystal can be useful for detector applications up to 216 °C.

3.3. Determination of dislocations density by chemical etching

Novotny and Moravec have studied dislocation densities in TGS crystal grown at 52 °C [20], whereas Chernov et al. present a general discussion on dislocations in solution grown crystals [21]. The (010) faces of LA-TGS crystals were etched using water as an etchant and examined under an optical microscope (Olympus U-TV0.5XC-3, Japan) in reflection mode. The comparative study was made on the LA-TGS crystals grown below and above T_c. Fig. 10(a) shows the etch pattern obtained on (010) face of LA-TGS crystal grown below T_c after etching with water for 5 s. Fig. 10(b) shows the etch pit pattern on (010) face of LA-TGS crystal grown by the SR method above T_c. The etching duration was kept same. The number of etch pits in the area of Fig. 10(a) and (b) is approximately equal to 40, which, with the area 0.20 cm × 0.15 cm of the photographs, gives the EPD = 1.3×10^3 cm^{-2}.

3.4. Piezoelectric studies

Piezoelectric crystals are widely used in surface acoustic wave (SAW) device applications [22]. Thin plates normal to [010] axis of LA-TGS crystal grown below and above T_c were cleaved for comparative measurement of piezoelectric coefficient (d_{33}). These samples were lapped and polished to get samples of 0.8 mm thickness. The samples were

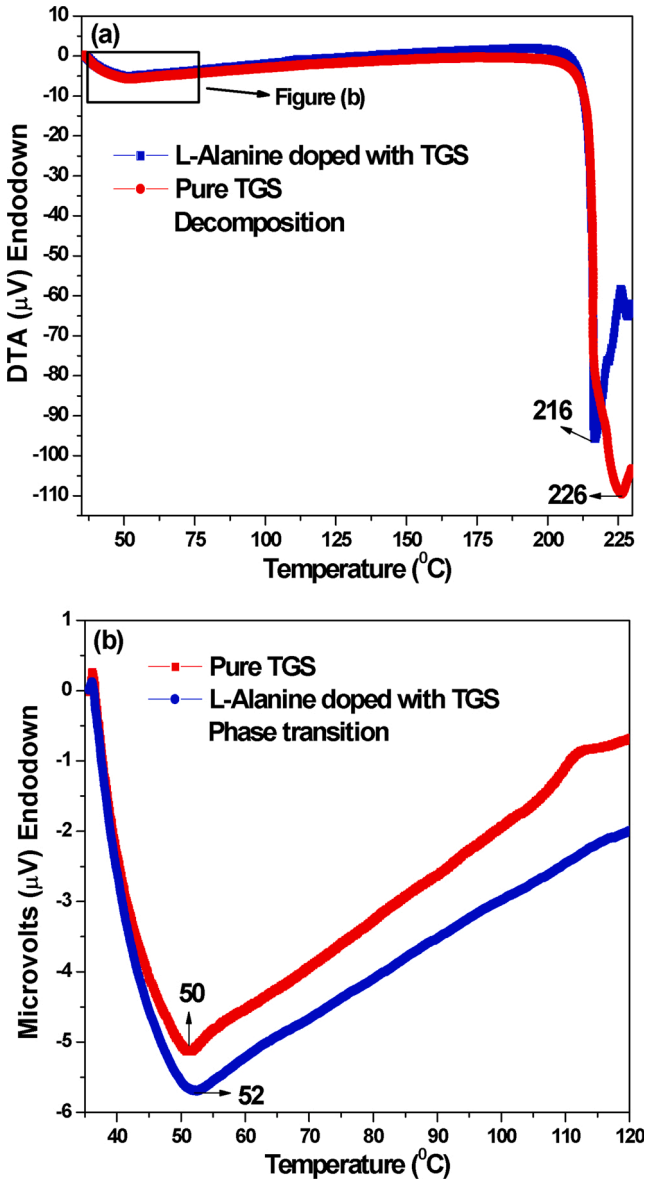

Fig. 9. Phase transition and decomposition temperature analysis using DTA.

coated with gold in the argon atmosphere on both sides to form electrodes using a sputtering unit (Emitech K 550X model). High precision digital Piezometer System was used to apply a calibrated force of 0.25 N at a frequency of 110 Hz at room temperature (30 °C), and the d_{33} coefficient was measured directly on an oscilloscope in the units of pC/N. The obtained d_{33} coefficients of LA-TGS crystals grown below and above T_c were 50 and 26 pC/N, respectively. The higher value of d_{33} for LA-TGS crystal grown below T_c than that grown above T_c is related to the concentration of point defects, because the point defects favour the formation of ferroelectric domains.

3.5. Dielectric permittivity and loss measurements

The samples of dimension 7 × 5×1 mm^3 were cut perpendicular to the b-axis from both the LA-TGS crystals. To make the surface conducting, gold electrodes were coated on the front and back sides of the samples. The dielectric studies on LA-TGS crystals grown below and above T_c were carried out in the frequency range 100 Hz to 1 MHz and in the temperature range 25 °C–65 °C using impedance/gain phase analyzer (Hewlett Packard 4194 A). The measurement was made while

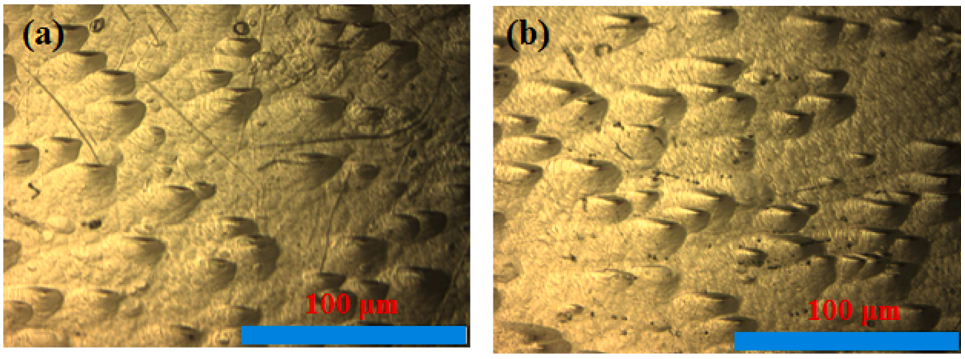

Fig. 10. Etch pits on (010) face of the LA-TGS crystals grown (a) below T_c and (b) above T_c after etching with water for 5 s.

cooling the sample at a rate of 1 °C/min in a furnace (DELTA 9023 model). It was observed that as the temperature of the crystal sample increases, the dielectric permittivity increases and shows a sharp rise around its Curie temperature i.e. phase transition temperature. Thereafter, it decreases sharply for both the LA-TGS crystals grown below and above T_c (Fig. 11(a, b)). It may be attributed to the fact that the process of domain nucleation proceeds up to Curie temperature, but beyond T_c, the polarization drops to zero as the existing dipoles lose their ordered states. The dielectric permittivity of LA-TGS crystal grown below T_c was found to be 430, whereas that of crystal grown above T_c was 1560, both at 100 Hz frequency (Fig. 11(b)). An important observation regarding the dielectric permittivity curve of LA-TGS crystal grown above T_c is that it is reasonably sharp whereas a strong broadening was observed in the permittivity curve for the LA-TGS crystal grown below T_c. The diffuseness of the dielectric curve could be attributed to the presence of large point defects in crystals grown below T_c as compared to the crystal grown above T_c. The defect-related local variation of phase transition temperature is well known in ferroelectrics [23]. More importantly, these defects restrict the domain wall mobility, therefore lowers the dielectric constant. The crystal grown above T_c has relatively fewer point defects, therefore undergo sharp anomaly near T_c with higher dielectric constant i.e. the domain walls are mobile enough to give higher dielectric constant. Another important feature in Fig. 11(a) is a slight shift in the phase transition temperature towards higher temperature for the crystal grown below T_c. It implies that the monoclinic phase became more stable and is retained until high temperatures. It is important to note that a shift in the transition temperature strongly depends on the type of point defects. For example, in $BaTiO_3$ based ferroelectric materials, it is well known that oxygen defects shift the transition temperature to the higher side whereas Ba i.e. A-site defects lower the transition temperature [24]. Because of this, it can be concluded that point defects generated in crystal grown below T_c are such that they increase phase transition temperature.

Fig. 12 shows the temperature-dependent dielectric loss (tan δ) at 100 Hz frequency for the LA-TGS crystals grown below and above T_c. The dielectric loss of LA-TGS crystals grown below and above T_c are 0.005 and 0.008, respectively. As discussed above, the relatively lesser

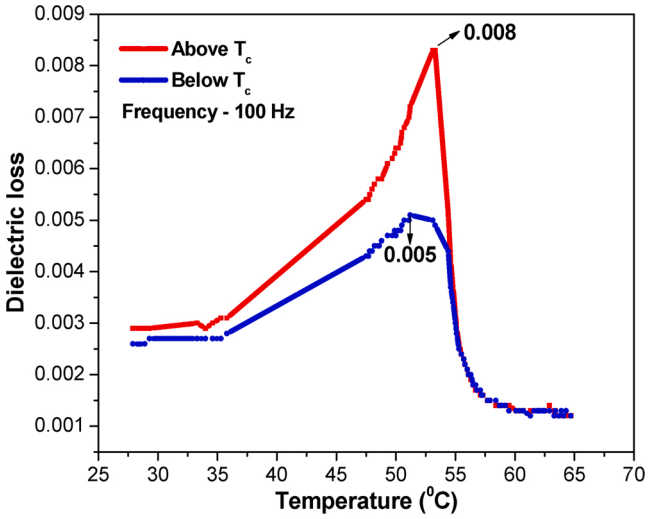

Fig. 12. Temperature dependent dielectric loss curve of the LA-TGS crystals grown below and above T_c.

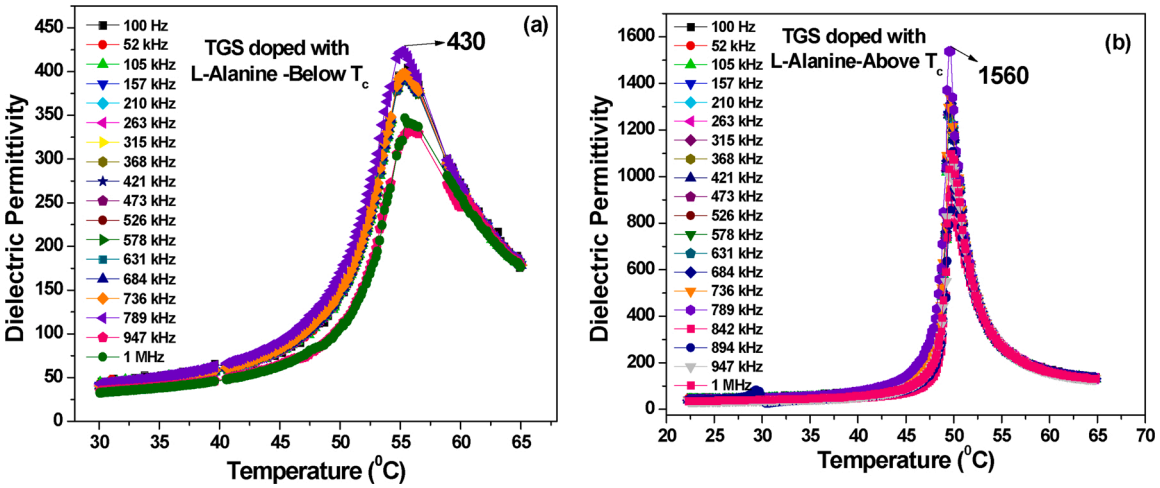

Fig. 11. Temperature dependent dielectric permittivity of the LA-TGS crystals grown (a) below T_c and (b) above T_c.

point defects in LA-TGS crystal grown above T_c and also due to domain wall friction results in higher dielectric loss as compared to crystal grown below T_c [25].

3.6. Optical transmittance

Optical quality is an important parameter for the device applications, such as in infrared (IR) detector fabrication. Optical transparency of LA-TGS crystals grown below and above T_c was measured by spectrophotometer (JASCO V-670) in the wavelength range from 190 nm to 2200 nm with slit width 2 nm and scan speed 200 nm/min. The beam was normal to (010) face of transparent crystal samples of 1 mm thickness. Fig. 13 shows the transmittance of 92 % and 80 % for LA-TGS crystals grown above and below T_c, respectively. Defects, particularly the point defects and volume defects (such as inclusions, bubbles, precipitates, etc.) affect the optical properties such as absorption, scattering, and refractive index, and therefore for device applications crystals free from these defects are required [26]. Since the crystal samples chosen for optical transmittance measurements do not have any visible volume defects, therefore high transmittance of LA-TGS crystal grown above T_c shows that it has low point defects due to the effect of growth conditions as compared to LA-TGS crystal grown below T_c.

Table 1 summarizes crystal growth parameters such as solubility, growth rates, etch pit density, piezoelectric, dielectric, and UV-Vis NIR transmittance of the LA-TGS crystals grown below and above T_c.

4. Conclusions

In the present study, ferroelectric crystals of L-alanine (7 mol %) doped triglycine sulphate (LA-TGS) oriented along [010] polar direction were grown below and above Curie temperature, and comparative investigations of their device relevant physical properties was performed. The salient results obtained are summarized below:

i Good quality, transparent, large size LA-TGS crystals oriented normal to (010) polar habit face were grown by unidirectional solution growth method in the ferroelectric and paraelectric temperature ranges. The grown crystal dimensions were: Length = 40 mm, Diameter = 30 mm in ferroelectric temperature range (below T_c) and Length = 50 mm and Diameter = 15 mm in paraelectric temperature range (above T_c).

ii The growth rate of the crystal grown below T_c was 1.3 mm/day and that grown above T_c was 3 mm/day.

iii Powder X-ray diffraction was used for phase confirmation, and the thermal studies show that the ferroelectric transition temperature of LA-TGS crystals is slightly higher than that reported for the pure TGS crystal.

iv The dislocations density measured by chemical etching for both the crystal was approximately same, and found to be equal to 1.3 $\times$ 10^3 cm^{-2}.

v The piezoelectric d_{33} coefficient of LA-TGS crystal grown below T_c was twice the value for the crystal grown above T_c.

vi The temperature-dependent dielectric studies show that the crystal grown below T_c has three times lower dielectric permittivity and low value of the dielectric loss, confirming that it is better for device applications than the crystal grown above T_c.

vii The UV-Vis-NIR optical transmittance for LA-TGS crystal grown below and above T_c was ~ 80 % and 92 %, respectively, showing the good optical quality of both the crystals.

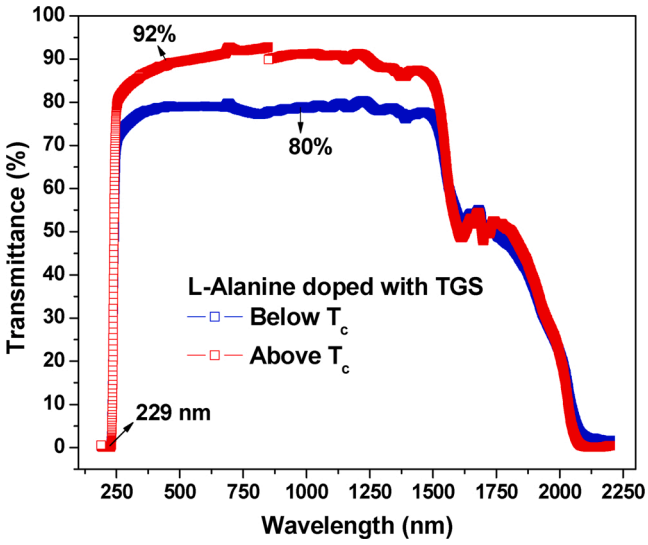

Fig. 13. UV-Vis NIR transmittance of the LA-TGS crystals grown below and above T_c.

Table 1
Summary of properties of [010] oriented LA-TGS crystals grown below and above T_c.

Property studied	LA-TGS crystal grown at 37 °C	LA-TGS crystal grown at 57 °C
Solubility	43 g/100 mL	75 g/100 mL
Growth rate	1.3 mm/day	3.0 mm/day
Etch Pit Density (EPD)	1.3 × 10^3 cm^{-2}	1.3 × 10^3 cm^{-2}
Piezoelectric (d_{33}) coefficient	50 pC/N	26 pC/N
Dielectric Permittivity	430	1560
Dielectric loss	0.005	0.008
UV–Vis-NIR transmittance	80 %	92 %

CRediT authorship contribution statement

Muthu Senthil Pandian: Methodology, Investigation, Data curation, Formal analysis, Supervision, Project administration, Writing - review & editing. **Sunil Verma:** Methodology, Investigation, Data curation, Formal analysis, Supervision, Project administration, Writing - review & editing. **P. Karuppasamy:** Methodology, Investigation, Data curation, Formal analysis, Supervision, Project administration, Writing - review & editing. **P. Ramasamy:** Methodology, Investigation, Data curation, Formal analysis, Supervision, Project administration, Writing - review & editing. **V.S. Tiwari:** Methodology, Investigation, Data curation, Formal analysis, Supervision, Project administration, Writing - review & editing. **A.K. Karnal:** Methodology, Investigation, Data curation, Formal analysis, Supervision, Project administration, Writing - review & editing.

Declaration of Competing Interest

The authors declare that they have no conflicts of interest.

Acknowledgements

M. Senthil Pandian is grateful to RRCAT authorities for six months project internship. G. Singh is acknowledged for help in the dielectric measurements.

References

[1] T. Tybell, C.H. Ahn, J.M. Triscone, Appl. Phys. Lett. 72 (1998) 1454.
[2] S. Satapathy, S.K. Sharma, A.K. Karnal, V.K. Wadhawan, J. Cryst. Growth 240 (2002) 196.
[3] J. Przeslawski, T. Iglesias, J.A. Gonzalo, Solid State Comm. 96 (1995) 195.
[4] R.W. Whatmore, Rep. Prog. Phys. 49 (1986) 1335.
[5] J.M. Herbert, Ferroelectric Transducers and Sensors, Gordon and Breach, New York, 1982.
[6] N. Nakatani, Jpn. J. Appl. Phys. 12 (1973) 1723.

[7] J.M. Chang, A.K. Batra, R.B. Lal, J. Cryst. Growth 158 (1996) 284.
[8] G. Arunmozhi, S. Lanceros Mendez, E.D. Matos Gomes, Mater. Lett. 54 (2002) 329.
[9] V.N. Shut, I.F. Kashevich, S.R. Syrtsov, Ferroelectrics 361 (2007) 113.
[10] H.V. Alexandru, C. Berbecaru, F. Stanculescu, L. Pintilie, I. Matei, M. Lisca, Sensors and Actuators A 113 (2004) 387.
[11] C.S. Fang, Y. Xi, Z.X. Chen, A.S. Bhalla, L.E. Cross, Mater. Lett. 2 (1983) 134.
[12] D. Panosova, S. Panos, Ferroelectrics 320 (2005) 59.
[13] J. Novotny, Z. Podvalova, J. Zelinka, Cryst. Growth Des. 3 (2003) 393.
[14] S. Dinakaran, Sunil Verma, S. Jerome Das, S. Kar, K.S. Bartwal, P.K. Gupta, Physica B 405 (2010) 1809.
[15] M. Senthil Pandian, N. Balamurugan, V. Ganesh, P.V. Raja Shekar, K. Kishan Rao, P. Ramasamy, Mater. Lett. 62 (2008) 3830.
[16] M. Senthil Pandian, P. Ramasamy, Binay Kumar, Mater. Res. Bull. 47 (2012) 1587.
[17] M. Senthil Pandian, Sunil Verma, P. Ramasamy, G. Singh, S.M. Gupta, V.S. Tiwari, A.K. Karnal, Appl. Phys. A 126 (2020) 492.
[18] M. Senthil Pandian, Sunil Verma, P. Karuppasamy, V. Padmanabhan, P. Ramasamy, V.S. Tiwari, A.K. Karnal, J. Cryst. Growth 546 (2020), 125793.
[19] M. Senthil Pandian, P. Ramasamy, J. Cryst. Growth 312 (2010) 413.
[20] J. Novotny, F. Moravec, J. Cryst. Growth 11 (1971) 329.
[21] A.A. Chernov, Chaps. 3, 6, and 9. Modern Crystallography III: Crystal Growth, Springer, Berlin, 1984.
[22] H. Takeda, K. Shimamura, T. Kohno, T. Fukuda, J. Cryst. Growth 169 (1996) 503.
[23] M.E. Lines, A.M. Glass, Principles and Applications of Ferroelectrics and Related Phenomena, Oxford University Press, Oxford, 2001.
[24] Y.S. Jung, E.S. Na, U. Paik, J. Lee, J. Kim, Mater. Res. Bull. 37 (2002) 1633.
[25] K.H. Hardtl, Ceram. Int. 8 (1982) 12.
[26] N.B. Singh, T.A. Gould, R.H. Hopkins, J. Cryst. Growth 78 (1986) 43.